Acta Oceanol. Sin., 2022, Vol. 41, No. 11, P. 23–33
https://doi.org/10.1007/s13131-021-1918-8
http://www.aosocean.com
E-mail: ocean2@hyxb.org.cn

Nutrient distributions and nitrogen-anomaly (N*) in the tropical North Pacific Ocean

Aiqin Han[1†], Yu Wang[1†], Yunlong Huo[1], Cai Lin[1], Kaiwen Zhou[1], Fangfang Kuang[1], Hui Lin[1*]

[1] Third Institute of Oceanography, Ministry of Natural Resources, Xiamen 361005, China

Received 11 May 2021; accepted 3 July 2021

Abstract

Based upon cruise observations broadly covering the tropical North Pacific during July–November 2017, together with data obtained from the World Ocean Circulation Experiment Hydrographic Program, this study examined the distribution of dissolved inorganic nitrogen (DIN, nitrate (NO_3^-)+nitrite (NO_2^-)), dissolved inorganic phosphorus (DIP) and related N* (nitrogen-anomaly, N*=N–16P+2.9, where N and P are the concentrations of DIN (>1.0 μmol/L) and DIP (>0.1 μmol/L)), used as an index of N_2 fixation, in the upper 1 000 m of the water column. Nutrient concentrations displayed distinct spatial variability in the upper ocean but became relatively constant at a depth of 1 000 m: they were high at low latitudes and in the eastern region, with an obvious nutricline at ~150 m (DIN, ~32.0 μmol/L; DIP, ~2.4 μmol/L) and then generally increased with depth; they decreased markedly (DIN, ~1.2 μmol/L; DIP, ~0.1 μmol/L; at ~150 m) at high latitudes and in the western region, where a nutricline was not apparent. The N* index showed significant meridional and zonal variation, with the most negative values located at low latitudes and in the eastern region (~10°N, ~150°–170°E), while becoming positive towards the northwest (the north of ~18°N, ~160°E westward). A N* concentration larger than 2.0 μmol/L which often used as an indicator of N_2 fixation, was observed between 155°E and 165°E; N* values were 2.0 μmol/L to 6.0 μmol/L at ~15°–28°N, i.e., much higher than those in the southern sector (0–2.0 μmol/L at ~5°–10°N). Zonally, N* decreased gradually from west (–2.0 μmol/L to 4.0 μmol/L, ~145°–165°E) to east (–2.0 μmol/L to –8.0 μmol/L, ~155°W) along ~10°N, which was consistent with the distribution of *Trichodesmium* abundance and N_2 fixation rates. Furthermore, since such region was also supplied with aeolian deposition, high N* was probably not only induced by N_2 fixation but also influenced by iron and/or nitrogen deposition.

Key words: tropical North Pacific Ocean, nutrients, nitrogen anomaly, nitrogen fixation, aeolian deposition

Citation: Han Aiqin, Wang Yu, Huo Yunlong, Lin Cai, Zhou Kaiwen, Kuang Fangfang, Lin Hui. 2022. Nutrient distributions and nitrogen-anomaly (N*) in the tropical North Pacific Ocean. Acta Oceanologica Sinica, 41(11): 23–33, doi: 10.1007/s13131-021-1918-8

1 Introduction

The tropical North Pacific is a critically important region affecting the global climate system, where water masses, heat and salt exchange actively, and is also under the influence of the western Pacific warm pool and the El Niño-Southern Oscillation (ENSO) (Hu et al., 2015; Liu et al., 2017). The region is characterized by low chlorophyll *a* concentration and low primary production relative to the other parts of the world ocean (Harrison et al., 1999; Ma et al., 2019), and this limitation in phytoplankton growth and production is attributed to its extremely low macronutrient levels (Kim et al., 2014; Matsumoto et al., 2016; Zhang et al., 2019b). Thus, careful examination of the nutrient distribution and nutrient concentration ratios is important to identify the limiting factors for this low production (Kim and Kim, 2013), yet nutrient data are still scarce in this oceanic region. Nutrient sources from nitrogen gas (N_2) fixation could also be important to support oceanic productivity in the subtropical gyres (Kitajima et al., 2009; Böttjer et al., 2016). However, the spatial patterns of N_2 fixation in this region are largely unknown due to the extreme lack of *in situ* observations.

Drawing from the classic sections of the Geochemical Ocean Sections Study (GEOSECS) (1972–1978) and World Ocean Circulation Experiment (WOCE) (1993–1994), Gruber and Sarmiento (1997) and Deutsch et al. (2001) adopted the quasi-conservative geochemical tracer N* (N*=N–16P+2.9) to investigate the distribution and rates of N_2 fixation and estimate the world ocean's nitrogen budget. Deutsch et al. (2001) also indicated that N_2 fixation rates were the highest, leading to an increase in nitrogen concentration and N* values in the Pacific Ocean compared to the Atlantic and Indian Oceans.

In the present study, nutrients and their ratios were investigated in a vast area of the tropical North Pacific during July to November 2017. By combining these with the nutrient data from the WOCE program, the distributions of dissolved inorganic nitrogen and phosphorus (DIN and DIP, respectively) were examined in the region and the spatial distribution of N* was evaluated, as this could be vital to understanding N_2 fixation dynamics. In addition, N* was related to the distribution of diazotrophs' abundance as well as aerosolized nitrogen and iron deposition to further identify the controlling factors for N_2 fixation in this region.

Foundation item: The Eastern Pacific Environment Monitoring and Protection Project under contract No. DY135-E2-5-02; the Global Change and Air-Sea Interaction Project; the National Natural Science Foundation of China under contract No. 42103077; the Natural Science Foundation of Fujian Province of China under contract No. 2020J05077.

*Corresponding author, E-mail: linhui@tio.org.cn

†These authors contributed equally to this work.

2 Materials and methods

2.1 *Study area*

The tropical North Pacific Ocean is characterized by complex interactions between the westward-flowing North Equatorial Current (NEC) along a latitude of ~13°–20°N, the eastward North Equatorial Countercurrent in the south, and the eastward North Pacific Subtropical Countercurrent in the north (Qiu et al., 2015; Liu et al., 2017). Throughout the year, the tropical North Pacific Ocean is oligotrophic, characterized by low nutrient concentration and low chlorophyll *a* concentration (Schlitzer, 2004; Cabrera et al., 2015), with DIN concentration ranging from <10.0 μmol/L to 2.5 μmol/L and DIP concentration <0.25 μmol/L in the upper 200 m at ~10°–30°N, while DIN concentration ranging from 2.0 μmol/L to 20.0 μmol/L and DIP concentration from 0.5 μmol/L to 2.0 μmol/L within 75–200 m depth at 5°–10°N. Chlorophyll *a* levels were <0.1–0.2 mg/m^3, with the subsurface chlorophyll maximum (SCM) layer located at ~100–150 m (Kitajima et al., 2009; Shiozaki et al., 2009).

2.2 *Sampling and measurements*

Field sampling in the present study covered 40 stations along two transects (Fig. 1): one was located at ~20°N, 155°–165°E, including a series of seamounts, i.e., Demao and Batiza, Niulang, and McDonnell Guyots; the other was located at ~10°N, 180°E–152°W, and included the China mining claim contract area (China Ocean Mineral Resources R&D Association contract area) and related deep-sea mining Clarion-Clipperton Zone. The cruise was conducted from July 12 to November 18, 2017 on board of the R/V *Xiangyanghong 03*.

Water samples from the upper 1 000 m were taken with 10 L Niskin bottles mounted onto a rosette sampler assembly, equipped with a conductivity-temperature-depth (CTD) recorder (SBE911 plus, Sea-Bird Co., USA). Nutrient samples were analyzed on board using standard methods. Nitrate (NO_3^-) and nitrite (NO_2^-) were determined by the pink azo dye method, and DIP was determined with the molybdenum blue method (Strickland and Parsons, 1972). The detection limits for NO_3^-, NO_2^-, and DIP analysis were 0.15 μmol/L, 0.06 μmol/L and 0.06 μmol/L, respectively. And the analytical precisions for the nutrients field measurements were better than 2.9% for NO_2^-, 4.2% for NO_3^-, and 3.1% for DIP, respectively. Since most of the ammonium concentrations in the open ocean were extremely low, normally less than 90.0 nmol/L (Zhu et al., 2018), the contribution of ammonium to DIN could be neglected for N* estimation.

Water samples (2 L) for analysis of *Trichodesmium* spp. were collected with Niskin bottles at different depths via CTD, specifically at 5 m, 50 m, 75 m, 100 m, 150 m, 200 m and the SCM layer. Samples were preserved in 4% buffered formalin for further analysis. In the land-based laboratory, the trichomes of *Trichodesmium* species were identified and counted using a Sedgewick Palmer Maloney chamber under a Zeiss Z1 inverted microscope (Germany) based on their morphological characteristics (Hynes et al., 2012). The abundance of *Trichodesmium* spp. was expressed as filament counts (filaments/L) regardless of the presence of colonial forms.

Aerosol samples were collected for aeolian nitrogen and iron deposition analysis in a parallel cruise and a prior cruise conducted from April 8 to May 8, 2017 on the R/V *Kexue*. Two large flow atmospheric particulate matter samplers (Lao Ying 2035, China) were installed on the compass deck (~15 m above sea level) to collect aerosol particles with a wind direction control system. Sampling conditions were such that the wind speed was >0.5 m/s, the relative wind direction was centered on the bow, and samples

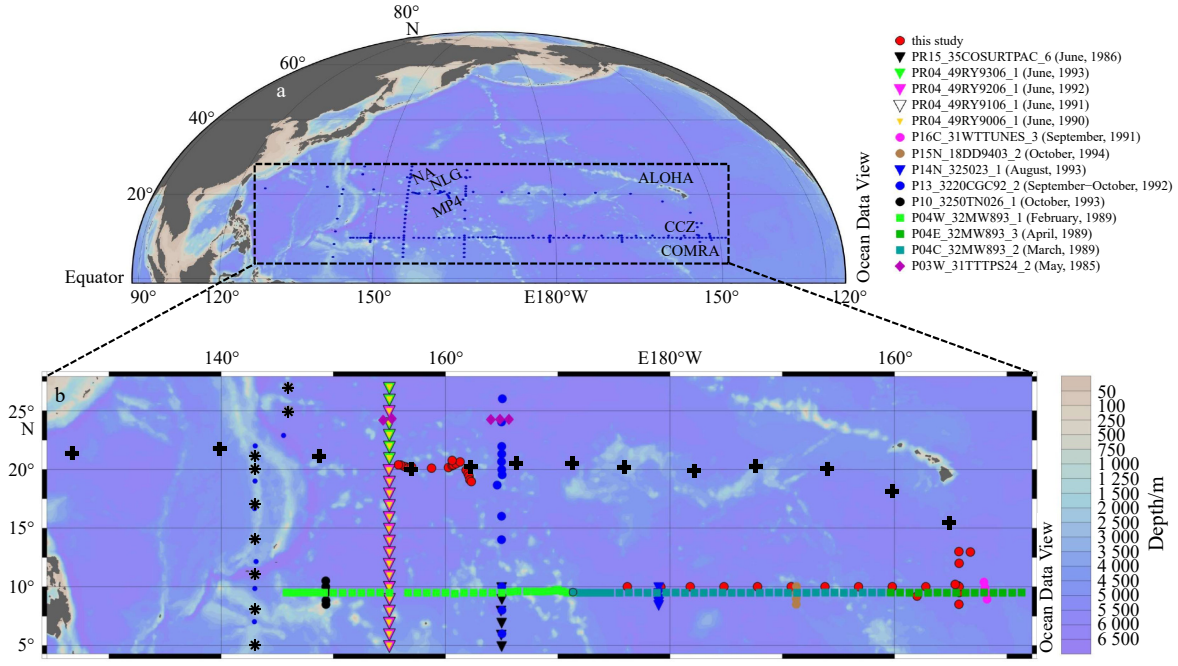

Fig. 1. Sampling locations in the tropical North Pacific Ocean based on the World Ocean Circulation Experiment (WOCE) program and our *in situ* cruise conducted from July 12 to November 18, 2017 (a, b). Stations for aerosol sampling conducted from April 8 to May 8, 2017 (black stars) and from July 19 to August 24, 2017 (black plus sign). Field sampling in the *in situ* cruise 2017 covered 40 stations (red dots with black circles) including a series of seamounts, i.e., Demao and Batiza (NA), Niulang (NLG), and McDonnell (MP4) Guyots, the China mining claim contract area (China Ocean Mineral Resources R&D Association contract area, COMRA) and related deep-sea mining Clarion-Clipperton Zone (CCZ). ALOHA: A Long-term Oligotrophic Habitat Assessment.

were collected when the wind direction was within 30 degrees. The samples for aeolian nitrogen (NO_3^-+NH_4^+) and dissolved iron (Fe_{DI}) deposition analysis were collected using cellulose acetate (Whatman 41) and quartz filters (Pall), respectively, and the filters were frozen and stored at –20°C. Aeolian nitrogen (μg/m^3) and Fe_{DI} (ng/m^3) were measured by ion chromatography (ICS-1600, Thermo Fisher, USA) and by inductivity coupled plasma-mass spectrometry (ICP-MS, Agilent 7700X, USA) (Piazzalunga et al., 2013; Shi et al., 2019). The analytical uncertainty was <2%. The dry deposition fluxes were roughly estimated as $F=V_d\times C_a$, where V_d is the dry deposition velocity and C_a is the atmospheric concentration of aerosol species. For simplicity, dry deposition velocities for individual species were assumed to be constant: 1.0 cm/s for NO_3^- (Luo et al., 2016), 0.1 cm/s for NH_4^+ (Luo et al., 2016), and 1.0 cm/s for Fe_{DI} (Chen et al., 2008; Baker et al., 2013), respectively.

2.3 *Data compilation*

To expand our understanding of the nutrient distribution and N*, as well as related large-scale nitrogen fixation (N_2 fixation) characteristics of the tropical North Pacific, hydrological and nutrient data from the WOCE Hydrographic Program (https://www.ewoce.org and https://cchdo.ucsd.edu/search?q=WOCE) were combined. WOCE data were scanned for outliers using the automatic and interactive methods of the Ocean Data View software (*_hy1.csvfiles from WOCE Hydrographic Program Office web-site as of May 27, 2002). The scanned WOCE data were downloaded from the Ocean Data View file, covering a spatial range ~5°–27°N, ~145°E –149°W (Table 1). Station locations are shown in Fig. 1, and data were obtained from the upper 1 000 m.

3 Results and discussion

3.1 *Hydrography of the tropical North Pacific Ocean*

Sectional distributions of potential temperature (θ) and salinity and the relationship between them in the tropical North Pacific are shown in Figs 2 and 3. The surface tropical North Pacific Ocean was occupied by North Pacific Tropical Surface Water (NPTSW) with high temperatures (~28.5°C) and a wide salinity range (~33.5–35.3) probably due to the influence of other water masses over the large coverage of the study area (Fig. 3). The latter may be mainly affected by the westward NEC with a strong speed of ~200 mm/s (Hu et al., 2015; Liu et al., 2017). Within the water column, θ generally decreased to ~5.0°C at 1 000 m depth in both latitudinal (along 155°E) and longitudinal (along 10°N) transects. The difference between two transects was that the 15°C isotherm showed a southward rise from ~400 m at 28°N to ~150 m at 10°N, which is consistent with the distribution of isopycnal of 25.0 kg/m^3 (Figs 2a, b, i and j). While the isotherm remained at ~150 m from ~150°–170°E to ~100 m and rose gradually to ~100–150 m at ~150°W (Fig. 2c). In contrast to θ, the salinity distribution was much more complex. Along 155°E, the maximum salinity (~35.3) appeared at the surface around 25°N and dropped abruptly to 200 m depth at 15°N, then rose slightly to 100–150 m at salinity of ~34.7, meanwhile, the density (σ_0) was within 23.0–24.0 kg/m^3 (Figs 2e, i), implying the water mixing between NPTSW and the North Pacific Central Water (NPCW) (Fig. 3). Along 10°N, this salinity maximum remained at 100–150 m at ~150°–170°E and rose to ~100 m at 160°W, outcropping at 150°W (Fig. 2g). This water mass with the maximum salinity was the NPCW (Pickard and Emery, 1990) (Fig. 3).

Under the maximum salinity layer, a water mass with low salinity of ~34.5 and high density of ~25.3–26.0 kg/m^3 appeared at 100–150 m at 150°W and inclined downward to ~250–300 m at 150°E (Figs 2g, h, k and l). This water mass, referred to as the California Current System (CCS), appears at low latitudes but not at high latitudes (north of ~13°N) (Tsuchiya, 1968). With increasing water depth, another water mass (salinity, ~34.8; σ_0, ~26.5–26.8 kg/m^3) was observed from 150°W (at ~200–500 m) to 150°E (at ~400 m), named the South Pacific Central Water (SPCW) (Sverdrup et al., 1942; Zhang et al., 2019a), which again only appeared at low latitudes (Fig. 2g, h, k and l). This water mass may be connected with the eastern tropical and South Pacific water mass (θ , ~8.0°C; salinity, ~34.75) with an oxygen minimum value <25.0 μmol/kg (Schlitzer, 2004).

At high latitudes (20°–25°N), North Pacific Intermediate Water (NPIW) with an extremely low salinity of ~34.2 and density of ~26.8 kg/m^3 was located at 500–800 m (Figs 2f, j). At water depths of ~1 000 m, Antarctic Intermediate Water (AAIW) was identified from its temperature of 5.0°C, salinity of 34.3–34.5, and density of ~27.4 kg/m^3 (Liu et al., 2017; Zhang et al., 2019a).

Table 1. Cruise information from the WOCE Hydrographic Program

Cruise	Cruise date
P03W_31TTTPS24_2	May 10, May 14–15, 1985
P04C_32MW893_2	March 9–21, 1989
P04E_32MW893_3	April 9–15, 1989
P04W_32MW893_1	February 28–March 1, February 23–24, February 19–March 4, 1989
P10_3250TN026_1	October 21–23, 1993
P13_3220CGC92_2	September 30–October 12, October 10, 1992
P14N_325 023_1	August 3–4, 1993
P15N_18DD9403_2	October 24–25, 1994
P16C_31WTTUNES_3	September 22–23, 1991
PR04_49RY9006_1	June 20–26, June 24–25, 1990
PR04_49RY9106_1	June 11–18, June 16–17, 1991
PR04_49RY9206_1	June 16, June 19, 1992
PR04_49RY9306_1	June 15–21, June 20, 1993
PR15_35COSURTPAC_6	June 26–27, 1986

3.2 *Distributions of DIN, DIP and nitrite*

Sectional distributions of DIN and DIP concentrations in the upper 1 000 m, and nitrite concentrations in the upper 200 m are shown in Fig. 4. Along 155°E, nutrients in the NPCW were extremely low, with DIN concentration less than 1.0 μmol/L and DIP concentration less than 0.1 μmol/L in the upper 100 m, and DIN and DIP concentrations of ~5.0 μmol/L and ~0.2 μmol/L, respectively, at 200 m depth (Figs 4a, e). With submergence of the NPCW, the DIN and DIP isolines of ~10.0 μmol/L and ~1.0 μmol/L, respectively, were located at ~400 m. Following the southward flow of the NPCW, the DIN and DIP isolines rose synchronously to ~150 m at low latitudes (~10°N). Thus, nutrients at low latitudes (~5°–10°N) showed a pronounced increase within the upper 200 m water column, as DIN and DIP concentrations increased from <1.0 μmol/L and <0.1 μmol/L at the surface (NPTSW) to ~23.0 μmol/L and ~1.8 μmol/L at 200 m (CCS). At high latitudes (~20°–25°N) nutrients increased gradually with increasing water depth, while at low latitudes (~10°N) nutrient concentrations increased markedly until they stabilized at 1 000 m where DIN and DIP concentrations attained ~38.0–45.0 μmol/L and ~2.8–3.3 μmol/L, respectively (Figs 4b, f).

Zonal nutrient distributions showed that they were dominated by a shift in water masses. Along 10°N, the NPTSW upper 100 m layer was again oligotrophic, with the same nutrient levels

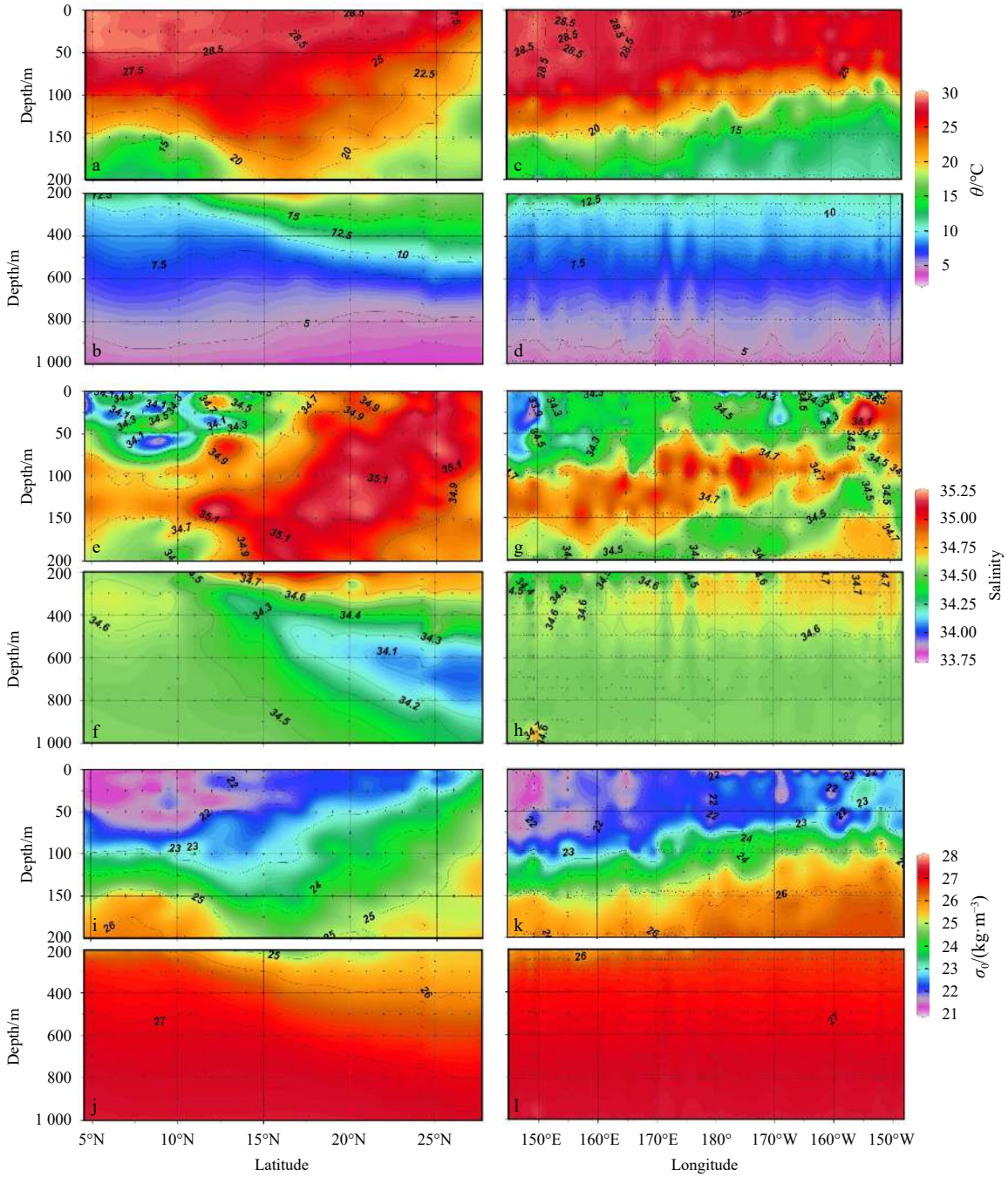

Fig. 2. Observed depth profiles of potential temperature (θ) (a–d), salinity (e–h), and density (σ_0) (i–l) of transects along ~155°E and ~10°N in the tropical North Pacific Ocean, including the dataset from the WOCE program and our *in situ* cruise in 2017.

as the meridional NPTSW. Within the NPCW water, nutrient DIN and DIP contour lines ranging from 5.0 μmol/L to 20.0 μmol/L and from 0.2 μmol/L to 1.5 μmol/L, respectively, lay between 125 m and 200 m in the western region (150°E), while the contour lines became noticeably shallower and thinner between 75 m and 100 m in the eastern region (150°W). Between 100 m and 200 m, nutrient concentrations in the SPCW water mass at 150°W increased noticeably and were as high as ~35.0 μmol/L and ~2.5 μmol/L for DIN and DIP, respectively (Figs 4c, g). In the western CCS water mass, similarly to the nutrient levels observed in the latitudinal CCS water mass, DIN concentrations were within 20.0–30.0 μmol/L and DIP concentrations between 1.5 μmol/L and 2.0 μmol/L. Since the AAIW occupied depths of ~1 000 m in the tropical North Pacific Ocean (Fig. 3), nutrient levels at longitudinal mid-deep water depth (~1 000 m) were comparable to those of latitudinal intermediate water as mentioned above (Figs 4d, h).

With respect to nitrite distributions, the maximum nitrite layer (MNL) became deeper, from ~100 m to ~200 m from 25°N to 20°N, corresponding to the NPCW submergence, with a concentration of ~0.15 μmol/L. Thereafter, the MNL became shallower at low latitudes (5°–10°N) with a higher nitrite concentration of 0.4 μmol/L at depths from ~75 m to ~125 m, consistent with the nutricline depth (Fig. 4i). Shallower MNL at 5°–10°N might be uplifted by southward flow of the NPCW. Zonally, nitrite concentrations along 10°N were comparable to those found along 155°E,

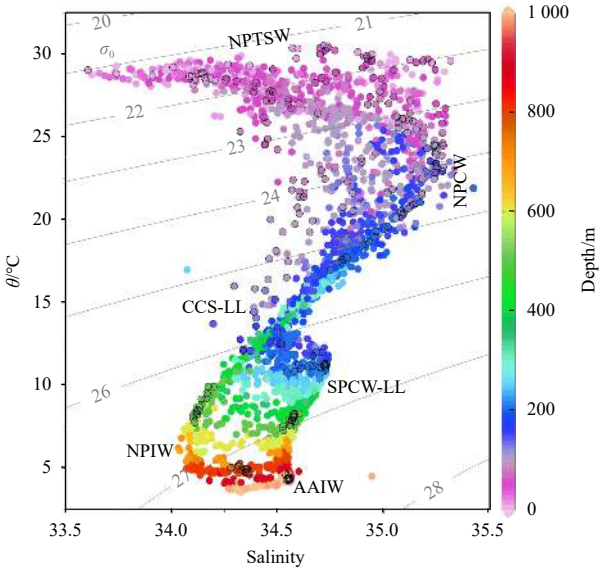

Fig. 3. Relationship between potential temperature(θ) and salinity in the tropical North Pacific Ocean showing observed water masses with depth indicated by colors, including data from the WOCE program (14 cruises listed in Table 1) and from our *in situ* cruise during August–November, 2017 (field data indicated by black circles). Isopycnal was indicated by grey lines. NPTSW, North Pacific Tropical Surface Water; NPCW, North Pacific Central Water; CCS-LL, California Current System waters observed at low latitudes (~13°N southward); SPCW-LL, South Pacific Central Water observed at low latitudes (~13°N southward); NPIW, North Pacific Intermediate Water; AAIW, Antarctic Intermediate Water.

with a value of ~0.3 μmol/L. The depth of the MNL was located at ~125 m and fluctuated between 75 m and 125 m. In contrast to the western region, the highest nitrite concentrations (0.6–0.8 μmol/L) occurred in the eastern tropical region (160°–150°W) at depths of 75–125 m (Fig. 4j), which indicated stronger nitrification in the eastern tropical Pacific Ocean compared to the western region.

3.3 *Nutrient dynamics as indicated by the relationship between DIN and DIP and the N-anomaly (N*)*

Nutrient dynamics, especially N_2 fixation, may be reflected by the variation in DIN/DIP concentration ratios and the N-anomaly, N* (Gruber and Sarmiento, 1997; Deutsch et al., 2001). Wong et al. (2007) also indicated that variation in N* could be influenced by the remineralization of organic matter. The N* index is defined as N*=N–16P+2.9 (Gruber and Sarmiento, 1997; Deutsch et al., 2001), where N and P are the concentrations of DIN (>1.0 μmol/L) and DIP (>0.1 μmol/L), respectively (Wong et al., 2007). The value of 2.9 is the global average deficit in nitrate resulting from denitrification (Wong et al., 2007).

The relationship between DIN and DIP is shown in Fig. 5. A linear relationship of DIN=14.21(±0.03)×DIP–1.31(±0.06) (coefficient of determination, r^2=0.992, n=4 162) , where DIN and DIP are the concentrations of DIN (μmol/L) and DIP (μmol/L), provided an excellent fit once all nutrient data were included. The slope of 14.2 was slightly lower than the classic Redfield ratio of 16:1 (Redfield et al., 1963), which provided a robust indication of nitrogen limitation. The DIN/DIP ratios varied with a clear latitudinal pattern that corresponded to the spatial variation of hydrological and nutrient distributions. As shown in Fig. 5, DIN/DIP ratios at high latitudes (north of ~20°N), where DIN and DIP concentrations were <25.0 μmol/L and <1.7 μmol/L respectively, systematically exceeded the ratios at southern latitudes with comparable nutrient levels. When DIN and DIP exceeded 25.0 μmol/L and 1.7 μmol/L, respectively, the meridional variation of DIN/DIP ratios clearly disappeared.

Examination of the molar vertical DIN/DIP ratios throughout the water column indicated that they ranged between 0.2 and 28 in the upper 200 m, and became stable and constant at ~14.2 at depths of 200–1 000 m (Figs 6a, c). Some high ratios of ~15:1–28:1 appeared at ~200 m at high latitudes; these were much higher than the fitted ratio of 14:1 (Fig. 5) and also apparently greater than the values (ranging from ~2 to 14) at southern latitudes (~5°–10°N) at ⩽200 m, as well as some of those determined at northern latitudes at ⩽200 m (Fig. 6a). Furthermore, DIN/DIP ratios at southern latitudes were between 2 and 14 and were concentrated in a relatively shallow layer of 75–120 m, while the ratios at northern latitudes were found at 150–200 m, corresponding to the nutricline distribution. Longitudinally, most DIN/DIP values in the eastern regions ranged between 2 and 14 in the shallower layer (⩽100 m), and remained constant (14:1) below 100 m. Further westward, at longitudes up to 150°E, the layer of DIN/DIP ratios between 5 and 14 became deeper, and was found at ~150 m, again attributable to the shallower nutricline (~100 m) in the eastern sector compared to that in the western sector (~150 m) (Fig. 6c). Below 200 m (to 1 000 m), both the latitudinal and longitudinal variation in DIN/DIP ratios became undetectable, maintaining a constant value of ~14.2 (Figs 6a, c).

Scatter plots of meridional and zonal N* water column distributions are shown in Figs 6b and d. In the upper 500 m, N* varied widely, with values ranging from –9.0 μmol/L to 5.0 μmol/L, while N* exhibited noticeably negative values (–8.0–0 μmol/L) below 500 m. Moreover, in the upper layer (⩽200 m), including the MNL where nitrification was most intense, N* varied conspicuously, with values ranging from –8.0 μmol/L to 6.0 μmol/L. In addition to the vertical N* variation, Fig. 6b shows the latitudinal and longitudinal difference in N*. Meridionally, N* values at high latitudes (>18°N) were significantly higher than those at low latitudes (<15°N) in the upper 600 m, and the meridional spatial variation became undetectable below 600 m. Furthermore, N* was much higher in the upper 500 m at northern latitudes, corresponding to the nutrient isohaline at ~600 m, with DIN and DIP concentrations of ~25.0 μmol/L and ~1.8 μmol/L, respectively, in the NPCW water mass (Figs 4b, f). Zonally, N* increased gradually from east (~150°W) to west (~150°E), with values ranging from –9.0 μmol/L to 0 μmol/L. The most negative N* value, located in the eastern Pacific Ocean at 500–600 m water depth, corresponded to the oxygen minimum zone characterized by a high denitrification rate (Gruber and Sarmiento, 1997). It is noteworthy that there was no obvious spatial difference in N* between 155°E and 165°E at northern latitudes (>18°N) throughout the water column, indicating that the maximum N* occurred in the Northwest Pacific.

As indicated earlier, the highly variable water column N* with both positive and negative values may be attributable to complex biogeochemical processes, i.e., nitrogen deposition (Kim et al., 2011, 2014; Kim and Kim, 2013), N_2 fixation (Capone et al., 2005; Bhavya et al., 2019), preferential uptake of DIP over DIN by phytoplankton (Clark et al., 2002) and/or nitrification of nitrogen-rich organic matter with an N:P ratio exceeding the Redfield ratio of 16 (Redfield et al., 1963; Singh et al., 2017). These negative N* values could also be explained by the preferential release

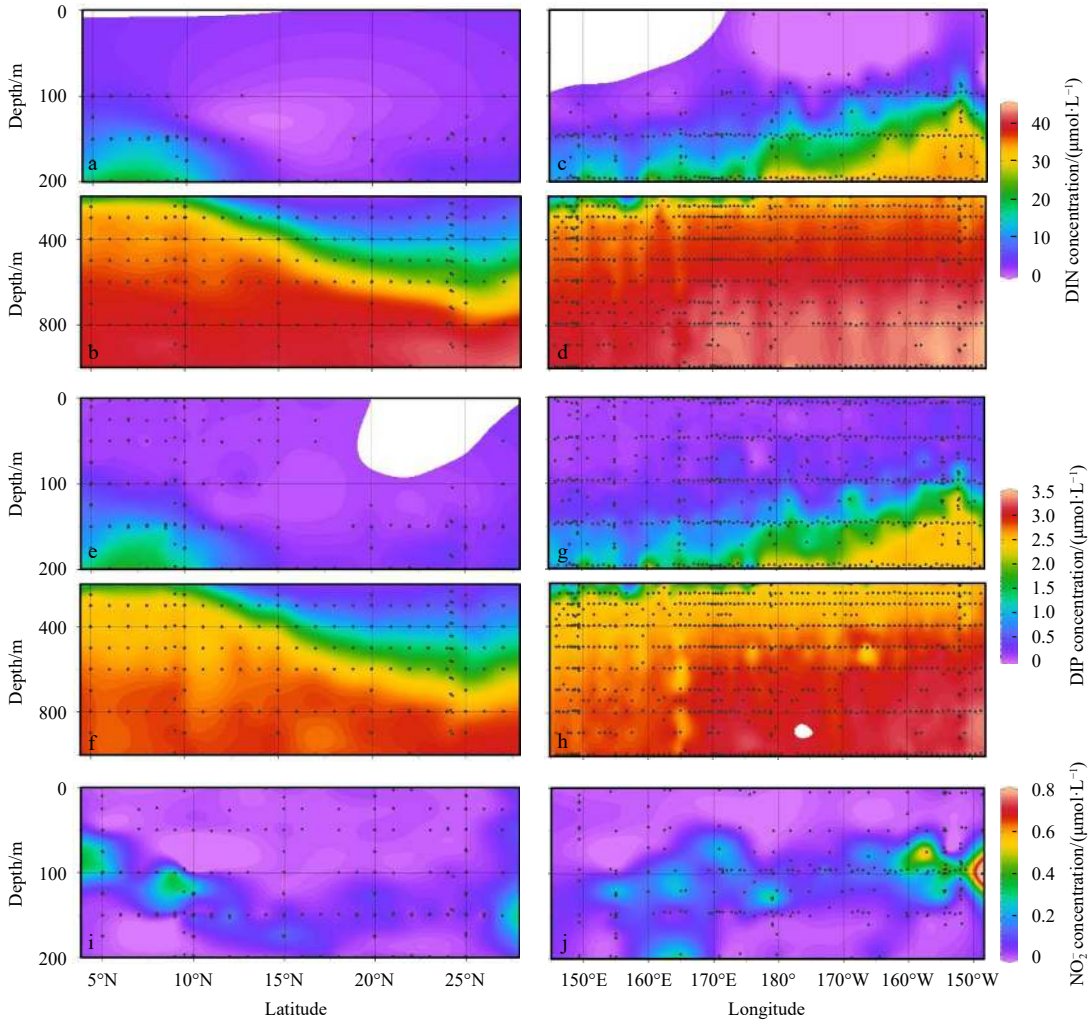

Fig. 4. Meridional and zonal distributions of dissolved inorganic nitrogen (DIN, a–d) and phosphorus (DIP, e–h) concentrations, respectively, in the upper 1 000 m. Meridional and zonal distributions of nitrite (NO_2^-) concentrations (i, j) in the upper 200 m along the 10°N and 155°E transects in the tropical North Pacific Ocean. Data were based on both WOCE dataset and our *in situ* cruise observations in 2017.

of DIP over DIN during particle remineralization (Hung et al., 2007).

Gruber and Sarmiento (1997) surveyed the N* distribution throughout the entire water column (0–6 000 m) in all major world oceans. They found that N* was less variable (ranging from −1.5 μmol/L to 1.0 μmol/L) in the Pacific region at 5°–25°N, ~170°E. Deutsch et al. (2001) further analyzed N* water column (0–6 000 m) data in the Pacific Ocean (along 180°E and 10°N) and suggested that N_2 fixation occurred primarily in the western Pacific subtropical gyres. Consistent with these results, and as shown in Fig. 6, in the present study the most positive N* values in the upper 500 m were located at northwestern stations (20°N northward, 165°E westward). Moreover, Zhang et al. (2019b) reported that N_2 fixation contributed an important N source which sustained 6.2%±3.7% of the primary production in the upper 200 m of the tropical North Pacific Ocean (13°–20°N, 120°–160°E). Recent studies indicated that the cyanobacterium *Trichodesmium* was one of the most important diazotrophs in the western tropical-subtropical Pacific Ocean (Chen et al., 2019). Kitajima et al. (2009) further demonstrated that microplanktonic diazotrophs were abundantly distributed in the North Pacific Ocean along a latitudinal gradient (with *Trichodesmium* spp. dominating at 26.5°N and *Richelia intracelluaris* around 8°N and 30°N). Thus, the present study focused on the N* data in the upper 200 m where a N_2 fixation signal was observed.

3.4 *Meridional and zonal N* characteristics in the upper 200 m water column*

As shown in Fig. 7a, along longitudes 155°E and 165°E, the N* maximum decreased from ~2.0 μmol/L at 5°N to ~0 μmol/L at 10°N. Thereafter, N* attained more positive values until it reached a maximum of 2.0–6.0 μmol/L at northern latitudes (15°–28°N), coinciding with a salinity front of the NPCW. It was acknowledged that mixing of water masses with different end-member values of N* might bias *in situ* estimated N* (Kim et al., 2014). As shown in Fig. S1a, the potential temperature-salinity diagram for the upper 200 m water column along 155°E and 165°E illustrated a three end-member mixing scheme. In order to separate the temporal N* trend from the contribution of physical mixing, a three end-member mixing model (Han et al., 2012; Kim et al., 2014) was adopted. This analysis was also performed along density coordinates σ_0 (~22.5–26.3 kg/m^3) for the core density layers of the main water masses. The N* addition signals (positive ΔN*, i.e., N sources larger than N sinks) from the isopycnal

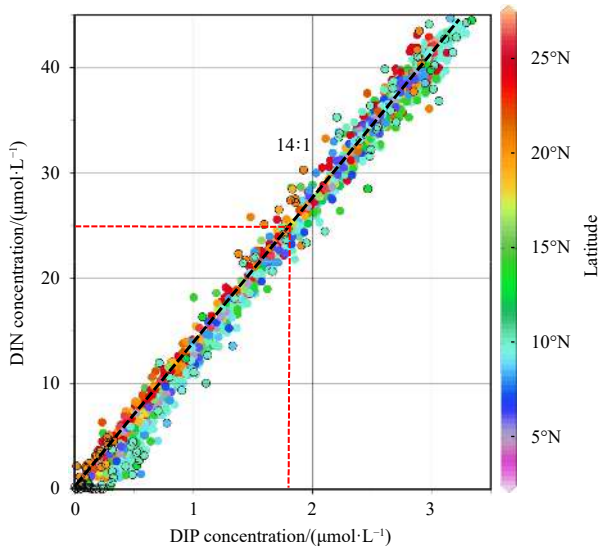

Fig. 5. Relationship between dissolved inorganic nitrogen and phosphorus, DIN and DIP, in the tropical North Pacific Ocean based on the WOCE dataset and *in situ* cruise data in 2017. Red dashed lines indicate the nutrient discrepancies in latitudinal variation, as DIN concentration ~25.0 μmol/L and DIP concentration ~1.7 μmol/L; 14:1 indicates the slope of the fitted linear regression.

analysis and θ-Salinity diagram was in good agreement with the latitudinal tendency for N* (Fig. S1b). Such consistency indicated that high N* along 155°E and 165°E was unlikely to be generated by physical mixing. This is also consistent with the previous study at northern Pacific Ocean which demonstrated that water mass mixing played a minor role for controlling the N* distribution in the upper water (Kim et al., 2014).

Given that N*>2.0 μmol/L have been proposed as indicators of N_2 fixation (Gruber and Sarmiento, 1997; Deutsch et al., 2001), we hypothesized that N_2 fixation, being one of the possible N sources, would occur with greater spatial variability and higher intensity at high latitudes than that at low latitudes.

The depth-integrated *Trichodesmium* abundance of 24.0 filaments/L at ~20°N, was ~4-fold higher than that at lower latitudes (~10°N) (Fig. 7a). It was in good agreement with the meridional N* distribution, suggesting that *Trichodesmium* spp. might dominate N_2 fixation during our cruise period. Although direct measurements of N_2 fixation rate were not obtained in the present study, the *Trichodesmium* abundance and N* signals obtained agreed well with the results of Kitajima et al. (2009). These authors found that the rate of N_2 fixation activity at northern latitudes (~15°–28°N) was ~4.0–8.0 nmol/(L·d) (in terms of N), and thus much greater than that at low latitudes (~1.0–5.0 nmol/(L·d) (in terms of N) at ~5°–15°N) (Fig. 7a). Kitajima et al. (2009) also reported that *Trichodesmium* spp. were the dominant microplanktonic diazotroph, contributing high N_2 fixation activity at 15°–28°N during their summer 2005 cruise, and Chen et al. (2019) demonstrated that *Trichodesmium* was the dominant N_2 fixing diazotroph in the western tropical Pacific Ocean.

Zonally, N* generally decreased from the west (ranging from 4.0 μmol/L to –2.0 μmol/L in ~145°–165°E) to the east (–2.0 μmol/L to –8.0 μmol/L at ~155°W) along ~10°N, except for the high N* values (0–4.0 μmol/L) recorded in 2017 (Fig. 7b). This longitudinal N* distribution was consistent with the distinct horizontal negative N* distribution at 200 m in the Pacific Ocean, which decreased from 2.0–4.0 μmol/kg to –10.0–12.0 μmol/kg from ~150°E to ~140°W (Gruber and Sarmiento, 1997). In the present study, a N* minimum (as low as ~15.0 μmol/kg, WOCE data) was also associated with the oxygen minimum zone in the SPCW water mass of the tropical eastern North Pacific Ocean (~200–600 m, Fig. 3). This water mass was also identified by Gruber and Sarmiento (1997) (Fig. 5 in their study) with N* as low as –7.0 μmol/L at ~200–600 m. This characteristic was associated with the N* distribution which at intermediate depths where low O_2 concentrations promoted denitrification processes and thus removed N (Kim et al., 2014). Again, the zonal depth-integrated *Trichodesmium* abundance demonstrated that the highest abundance (~18.0 filaments/L) coincided with the highest positive N* value at ~160°W, and the abundance decreased eastward thereafter. Taken together, these findings suggest that *Trichodesmium* spp. actively contributed to N_2 fixation in the tropical North Pacific euphotic layer and that these cells were distributed with a distinct pattern of spatial variability.

It has been recognized that high N* in the tropical northwest Pacific Ocean might not only be associated with N_2 fixation activity (Gruber and Sarmiento, 1997; Deutsch et al., 2001), but also with aeolian dust deposition which appeared to play a critical role in N_2 fixation and the nitrogen budget (Karl et al., 2002; Kim et al., 2011, 2014; Kim and Kim, 2013). The latter studies suggested that the spatial pattern and absolute magnitude of the rate of increase of N* at mid-latitudes (20°–40°N) in the North Pacific agreed well with the atmospheric nitrogen deposition rates derived from an atmospheric transport model and observations. Aerosol nitrogen deposition in the tropical North Pacific was determined in the present study and in a prior cruise (April–May 2017) in which the sampling sites were close to the nutrient sampling stations (Figs 1 and 7a). As shown in Fig. 7a, within ~143°–146°E, the aerosol nitrogen deposition flux was relatively constant at ~3.0–5.0 μmol/(m²·d) between 5°–25°N in April–May 2017, and was enhanced at ~28°N with maxima of ~16.0 μmol/(m²·d), that agreed well with the high N* at 15°–28°N (Fig. 7a). Similar to the meridional consistence between nitrogen deposition and N* distributions, the longitudinal nitrogen deposition agreed well with the eastward decreasing N* distribution. Nitrogen deposition was extremely high in the western North Pacific, with a maximum of ~28.0 μmol/(m²·d) at ~130°E in July–August 2017, and then decreased markedly to ~6.0 μmol/(m²·d) at ~160°W (Fig. 7b). The agreement between meridional and zonal nitrogen deposition rates and the N* distribution, indicates that aerosol nitrogen deposition could also cause the observed DIN elevation and high N* signals in the upper layer of the tropical North Pacific.

Taken together, the field atmospheric nitrogen deposition rate was (7.85±6.51) μmol/(m²·d) (in terms of N) (Fig. 7a), which agreed well with the model result of 5.5–16.4 μmol/(m²·d) (in terms of N) (Kim et al., 2014). The field N_2 fixation rate was (0.60±0.96) nmol/(L·d) (in terms of N) (Kitajima et al., 2009), which could be estimated as (120±192) μmol/(m²·d) (in terms of N) in the upper 200 m. Such an estimation was in the same order with the results from Zhang et al. (2019b). Thus, the N_2 fixation rate was larger than atmospheric deposition per unit area. On the other hand, it has been reported that modeled N deposition was ~7.0 Tg/a in the North Pacific Ocean, ~7.5 Tg/a in the North Central Pacific Ocean, and ~6.9 Tg/a in Equatorial Pacific Ocean (Okin et al., 2011). Geometric mean depth-integrated N_2 fixation rates in tropical North Pacific Ocean were ~20–120 μmol/(m²·d) and the North Pacific Ocean area was thus assumed to be ~8.9×

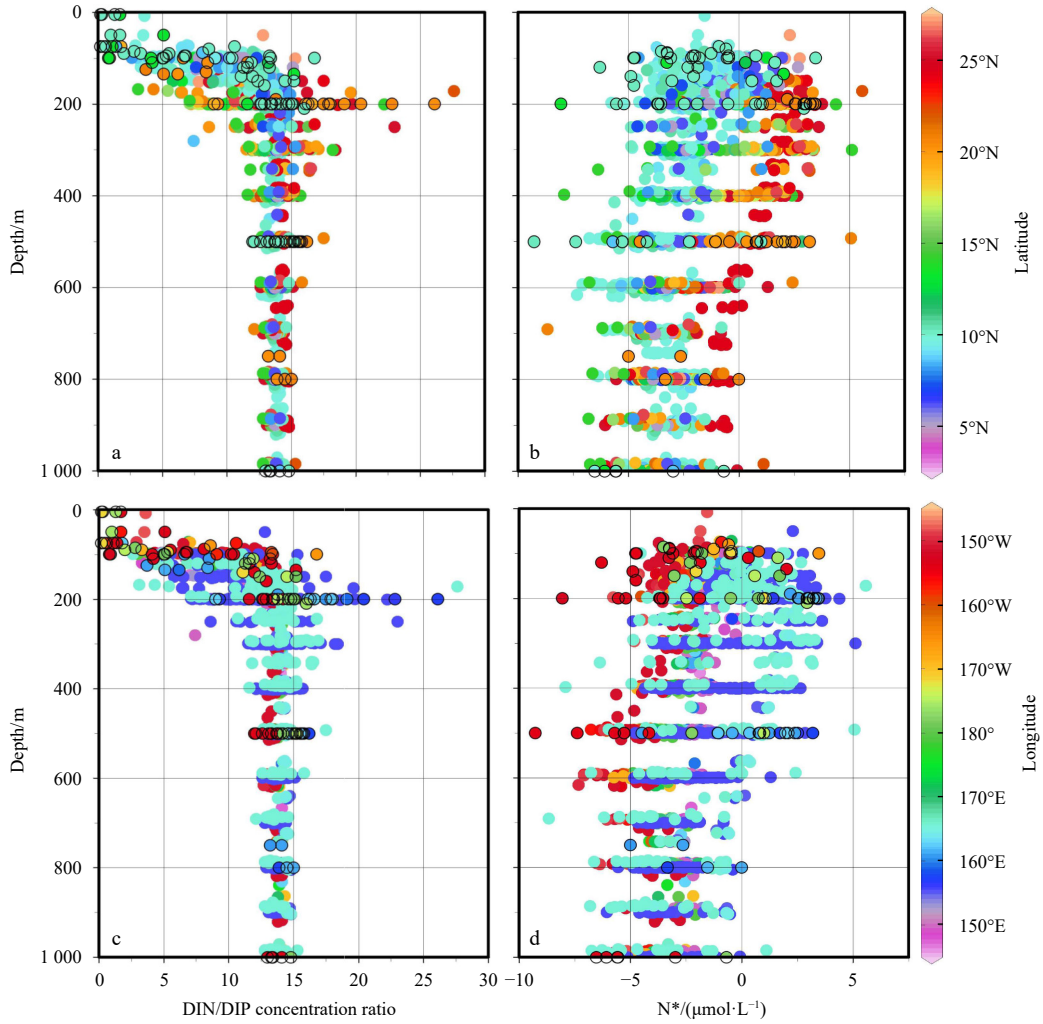

Fig. 6. Vertical water column depth distribution of DIN/DIP concentration ratios and nitrogen anomaly (N*) in the tropical North Pacific Ocean. Black circles represent *in situ* data from the 2017 cruise, the remainder correspond to the WOCE program.

10^{13} m^2 (Luo et al., 2012), the N_2 fixation flux was calculated to be ~9.1–54.6 Tg/a. It seemed again that N_2 fixation contribution was higher relative to atmospheric deposition.

Moreover, the rate of aeolian Fe_{DI} flux displayed a similar pattern to that of nitrogen deposition (Fig. 7a), remaining constant at ~10.0 nmol/(m^2·d) within 5°–25°N in April–May 2017 and increasing to ~110.0 nmol/(m^2·d) at ~28°N, again in good agreement with the elevated N* distributions at high latitudes. Zonally, the aerosol Fe_{DI} was consistent with nitrogen deposition, decreasing from ~42.0 nmol/(m^2·d) in the western ocean to ~8.0 nmol/(m^2·d) in the eastern ocean (Fig. 7b). Although nitrogen deposition may be attributable to the high N* in the study area, aeolian Fe_{DI} deposition might play an important synchronous role in the distribution of *Trichodesmium* spp. and thus strongly influence their N_2 fixation activity in the tropical North Pacific Ocean.

4 Conclusions

Based on the WOCE dataset and results of the 2017 *in situ* cruises, the present study identified nutrient characteristics associated with hydrological features across the large tropical North Pacific Ocean area, and investigated meridional and zonal N* distributions, finding the highest positive N* value (2.0–6.0 μmol/L) in the northwest region (~15°–25°N, ~155°–165°E) (a N*>2.0 μmol/L is considered an indicator of N_2 fixation activity). *Trichodesmium* spp. were the dominant contributor to N_2 fixation during the sampling period and their depth-integrated abundance was the highest in the northwest Pacific Ocean, where high N_2 fixation rate has been observed. Results of this study confirmed that such spatial variation in the N* index may not only be induced by N_2 fixation, but also by aeolian nitrogen and iron deposition. The former may elevate nitrogen concentrations and thus N* in the upper water column, and the latter may play an important role in the distribution of diazotrophs and enhanced N_2 fixation.

Although N* distributions in this study were roughly consistent with the distributions of N-fixing cyanobacteria and those of aerosol nitrogen and iron deposition, the field-determined meridional and zonal N_2 fixation activity and abundance and distribution of specific diazotrophs are still not adequately quantified. Furthermore, the tropical North Pacific Ocean is oligotrophic, with nutrient concentrations at the nanomolar per litre level, and it is critical to determine DIN/DIP ratios and the related N* in the upper column. Additionally, the importance of aeolian dust deposition, including that of nitrogen and iron in elevating the N* signal, remain poorly definition. Taken together, results of this study highlight the variability in the meridional and zonal N_2 fixation. Additional field studies are needed, however, to improve on the spatial characterization of N_2 fixation and associated nitrogen budgets.

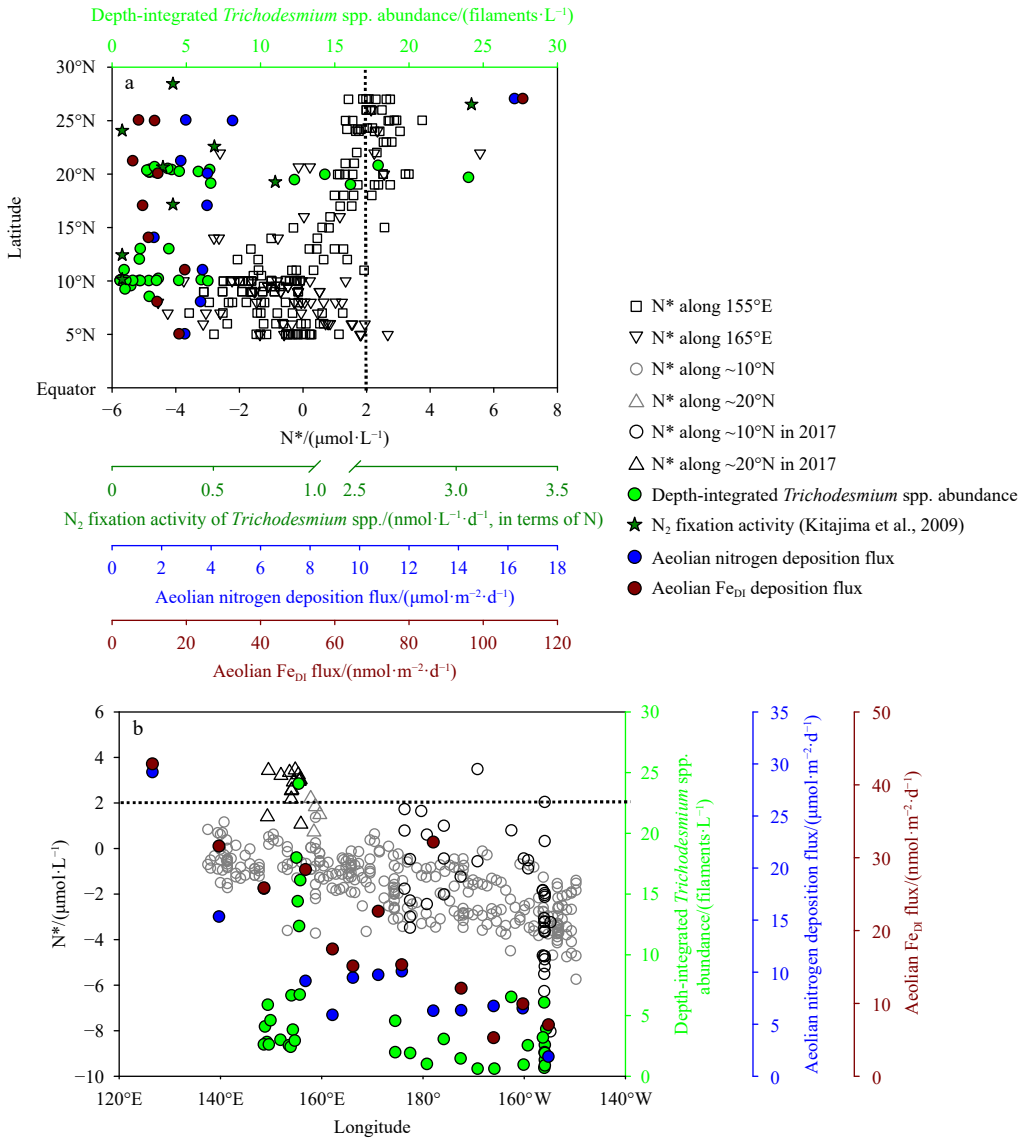

Fig. 7. Meridional (along ~155°E and ~165°E) (a) and zonal (along ~10°N and ~20°N) (b) water column depth sections of the nitrogen anomaly (N*, μmol/L) in the upper 200 m of the tropical North Pacific Ocean based on WOCE data and *in situ* data from the 2017 cruise. Depth-integrated *Trichodesmium* spp. abundance in the upper 200 m is represented by green dots; N_2 fixation activity of *Trichodesmium* spp. along 155°E measured according to Kitajima et al. (2009) is represented by dark green stars. Latitudinal and longitudinal fluxes of aeolian nitrogen and Fe_{DI} deposition were obtained in April–May 2017 and July–August 2017, respectively.

Acknowledgements

This study was partially supported by the numerous National Science Foundation grants under the WOCE program. We thank all the scientists and technicians involved in data collection and analysis of the high quality data from the WOCE program. We also thank the captain and crew of the R/V *Xiangyanghong 03* and R/V *Kexue* for their assistance while sampling at sea.

References

Baker A R, Adams C, Bell T G, et al. 2013. Estimation of atmospheric nutrient inputs to the Atlantic Ocean from 50°N to 50°S based on large-scale field sampling: iron and other dust-associated elements. Global Biogeochemical Cycles, 27(3): 755–767, doi: 10.1002/gbc.20062

Bhavya P S, Min J O, Kim M S, et al. 2019. A review on marine N_2 fixation: mechanism, evolution of methodologies, rates, and future concerns. Ocean Science Journal, 54(4): 515–528, doi: 10.1007/s12601-019-0037-3

Böttjer D, Dore J E, Karl D M, et al. 2016. Temporal variability of nitrogen fixation and particulate nitrogen export at Station ALOHA. Limnology and Oceanography, 62(1): 200–216

Cabrera O C, Villanoy C L, Alabia I D, et al. 2015. Shifts in chlorophyll *a* off Eastern Luzon, Philippines, associated with the North Equatorial Current bifurcation latitude. Oceanography, 28(4): 46–53, doi: 10.5670/oceanog.2015.80

Capone D G, Burns J A, Montoya J P, et al. 2005. Nitrogen fixation by *Trichodesmium* spp. : an important source of new nitrogen to the tropical and subtropical North Atlantic Ocean. Global Biogeochemical Cycles, 19(2): GB2024, doi: 10.1029/2004GB002331

Chen Mingming, Lu Yangyang, Jiao Nianzhi, et al. 2019. Biogeographic drivers of diazotrophs in the western Pacific Ocean. Limnology and Oceanography, 64(3): 1403–1421, doi: 10.1002/lno.11123

Chen Ying, Paytan A, Chase Z, et al. 2008. Sources and fluxes of atmospheric trace elements to the Gulf of Aqaba, Red Sea. Journal of Geophysical Research, 113(D5): D05306, doi: 10.1029/2007JD

009110

Clark D R, Flynn K J, Owens N J P. 2002. The large capacity for dark nitrate-assimilation in diatoms may overcome nitrate limitation of growth. New Phytologist, 155(1): 101–108, doi: 10.1046/j.1469-8137.2002.00435.x

Deutsch C, Gruber N, Key R M, et al. 2001. Denitrification and N_2 fixation in the Pacific Ocean. Global Biogeochemical Cycles, 15(2): 483–506, doi: 10.1029/2000GB001291

Gruber N, Sarmiento J L. 1997. Global patterns of marine nitrogen fixation and denitrification. Global Biogeochemical Cycles, 11(2): 235–266, doi: 10.1029/97GB00077

Han Aiqin, Dai Minhan, Kao Shuh-Ji, et al. 2012. Nutrient dynamics and biological consumption in a large continental shelf system under the influence of both a river plume and coastal upwelling. Limnology and Oceanography, 57(2): 486–502, doi: 10.4319/lo.2012.57.2.0486

Harrison P J, Boyd P W, Varela D E, et al. 1999. Comparison of factors controlling phytoplankton productivity in the NE and NW subarctic Pacific gyres. Progress in Oceanography, 43(2–4): 205–234

Hu Dunxin, Wu Lixin, Cai Wenju, et al. 2015. Pacific western boundary currents and their roles in climate. Nature, 522(7556): 299–308, doi: 10.1038/nature14504

Hung J J, Wang S M, Chen Y L. 2007. Biogeochemical controls on distributions and fluxes of dissolved and particulate organic carbon in the northern South China Sea. Deep-Sea Research Part II: Topical Studies in Oceanography, 54(14–15): 1486–1503, doi: 10.1016/j.dsr2.2007.05.006

Hynes A M, Webb E A, Doney S C, et al. 2012. Comparison of cultured *Trichodesmium* (Cyanophyceae) with species characterized from the field. Journal of Phycology, 48(1): 196–210, doi: 10.1111/j.1529-8817.2011.01096.x

Karl D, Michaels A, Bergman B, et al. 2002. Dinitrogen fixation in the world's oceans. Biogeochemistry, 57(1): 47–98, doi: 10.1023/A:1015798105851

Kim T H, Kim G. 2013. Changes in seawater N: P ratios in the northwestern Pacific Ocean in response to increasing atmospheric N deposition: results from the East (Japan) Sea. Limnology and Oceanography, 58(6): 1907–1914, doi: 10.4319/lo.2013.58.6.1907

Kim I N, Lee K, Gruber N, et al. 2014. Increasing anthropogenic nitrogen in the North Pacific Ocean. Science, 346(6213): 1102–1106, doi: 10.1126/science.1258396

Kim T W, Lee K, Najjar R G, et al. 2011. Increasing N abundance in the northwestern Pacific Ocean due to atmospheric nitrogen deposition. Science, 334(6055): 505–509, doi: 10.1126/science.1206583

Kitajima S, Furuya K, Hashihama F, et al. 2009. Latitudinal distribution of diazotrophs and their nitrogen fixation in the tropical and subtropical western North Pacific. Limnology and Oceanography, 54(2): 537–547, doi: 10.4319/lo.2009.54.2.0537

Liu Zhiyu, Lian Qiang, Zhang Fangtao, et al. 2017. Weak thermocline mixing in the North Pacific low-latitude western boundary current system. Geophysical Research Letters, 44(20): 10530–10539, doi: 10.1002/2017GL075210

Luo Yawei, Doney S C, Anderson L A, et al. 2012. Database of diazotrophs in global ocean: abundance, biomass and nitrogen fixation rates. Earth System Science Data, 4(1): 47–73, doi: 10.5194/essd-4-47-2012

Luo Li, Yao Xiaohong, Gao Huiwang, et al. 2016. Nitrogen speciation in various types of aerosols in spring over the northwestern Pacific Ocean. Atmospheric Chemistry and Physics, 16(1): 325–341, doi: 10.5194/acp-16-325-2016

Ma Jun, Song Jinming, Li Xuegang, et al. 2019. Environmental characteristics in three seamount areas of the tropical western Pacific Ocean: focusing on nutrients. Marine Pollution Bulletin, 143: 163–174, doi: 10.1016/j.marpolbul.2019.04.045

Matsumoto K, Abe O, Fujiki T, et al. 2016. Primary productivity at the time-series stations in the northwestern Pacific Ocean: is the subtropical station unproductive?. Journal of Oceanography, 72(3): 359–371, doi: 10.1007/s10872-016-0354-4

Okin G S, Baker A R, Tegen I, et al. 2011. Impacts of atmospheric nutrient deposition on marine productivity: roles of nitrogen, phosphorus, and iron. Global Biogeochemical Cycles, 25(2): GB2022, doi: 10.1029/2010GB003858

Piazzalunga A, Bernardoni V, Fermo P, et al. 2013. Optimisation of analytical procedures for the quantification of ionic and carbonaceous fractions in the atmospheric aerosol and applications to ambient samples. Analytical and Bioanalytical Chemistry, 405(2): 1123–1132

Pickard G L, Emery W J. 1990. Descriptive Physical Oceanography: An Introduction. 5th ed. Oxford: Pergamon Press

Qiu Bo, Rudnick D L, Cerovecki I, et al. 2015. The Pacific north equatorial current: new insights from the origins of the Kuroshio and Mindanao Currents (OKMC) Project. Oceanography, 28(4): 24–33, doi: 10.5670/oceanog.2015.78

Redfield A C, Ketchum B H, Richards F A. 1963. The influence of organisms on the composition of sea-water. In: Hill M N, ed. The Sea. New York: Interscience, 26–77

Schlitzer R. 2004. Export production in the equatorial and North Pacific derived from dissolved oxygen, nutrient and carbon data. Journal of Oceanography, 60(1): 53–62, doi: 10.1023/B:JOCE.0000038318.38916.e6

Shi Jinhui, Wang Nan, Gao Huiwang, et al. 2019. Phosphorus solubility in aerosol particles related to particle sources and atmospheric acidification in Asian continental outflow. Atmospheric Chemistry and Physics, 19(2): 847–860, doi: 10.5194/acp-19-847-2019

Shiozaki T, Furuya K, Kodama T, et al. 2009. Contribution of N_2 fixation to new production in the western North Pacific Ocean along 155°E. Marine Ecology Progress Series, 377: 19–32, doi: 10.3354/meps07837

Singh A, Bach L T, Fischer T, et al. 2017. Niche construction by non-diazotrophs for N_2 fixers in the eastern tropical North Atlantic Ocean. Geophysical Research Letters, 44(13): 6904–6913, doi: 10.1002/2017GL074218

Strickland J D H, Parsons T R. 1972. A Practical Handbook of Seawater Analysis. 2nd ed. Ottawa: Fisheries Research Board of Canada

Sverdrup H U, Fleming R H, Johnson M W. 1942. The Oceans, Their Physics, Chemistry, and General Biology. New York: Prentice-Hall

Tsuchiya M. 1968. Upper Waters of the Intertropical Pacific Ocean. Baltimore: Johns Hopkins Press, 1–50

Wong G T F, Tseng C M, Wen Liang-Saw, et al. 2007. Nutrient dynamics and N-anomaly at the SEATS station. Deep-Sea Research Part II: Topical Studies in Oceanography, 54(14–15): 1528–1545

Zhang Lei, Tian Yongqing, Pan Aijun, et al. 2019a. Analysis of water masses at the 10°N section in the tropical central and eastern Pacific. Haiyang Xuebao (in Chinese), 41(11): 40–50

Zhang Run, Zhang Dongsheng, Chen Min, et al. 2019b. N_2 fixation rate and diazotroph community structure in the western tropical North Pacific Ocean. Acta Oceanologica Sinica, 38(12): 26–34, doi: 10.1007/s13131-019-1513-4

Zhu Yifan, Liu Jing, Huang Tao, et al. 2018. On the fluorometric measurement of ammonium in oligotrophic seawater: assessment of reagent blanks and interferences. Limnology and Oceanography, 16(8): 516–524

Supplementary information:

Fig. S1. The potential temperature (θ) (°C) vs. salinity scheme in the upper 200 m water column along 155°E and 165°E in the tropical North Pacific Ocean (a); ΔN* distributions vs. latitude diagram in the upper 200 m water column along 155°E and 165°E (b).

Table S1. Properties of end member water masses and derived ΔN* included in the upper 200 m water column along 155°E and 165°E.

Text S1. The calculation for the physical mixing on N*.

The supplementary information is available online at https://doi.org/10.1007/s13131-021-1918-8 and http://www.aosocean.com/. The supplementary information is published as submitted, without typesetting or editing. The responsibility for scientific accuracy and content remains entirely with the authors.